

Single Axis Automatic Sun Tracking System based on Fuzzy Logic Control

G. Sundar and D. Sathish

Department of Electrical and Electronics Engineering,
Arulmigu Meenakshi Amman College of Engineering,
Kanchipuram, Tamil Nadu, India

Copyright © 2016 ISSR Journals. This is an open access article distributed under the *Creative Commons Attribution License*, which permits unrestricted use, distribution, and reproduction in any medium, provided the original work is properly cited.

ABSTRACT: This paper proposes a single stage current source inverter based photovoltaic system with single axis automatic sun tracking system. The system consists of transformer less single stage conversion for tracking the maximum power point which is maintained by a fuzzy logic controller. The Hardware system presents the fuzzy logic control based sun tracking system using an Arduino controller. To improve the power quality and system efficiency, a double-tuned parallel resonant circuit is added to eliminate the 2nd and 4th order harmonics at the inverter side. A Stepper motor aids in tracking the sun axis and keeps the panel in line direction with sun all day long. The efficiency of the solar cells has been enhanced by the proposed design system. The proposed fuzzy logic controller has been implemented and tested using MATLAB Simulink environment. Moreover, the said sun tracking power generation system has been tested in real time using an Arduino controller.

KEYWORDS: Maximum power point tracking, Arduino controller, Fuzzy logic controller, Power quality.

1 INTRODUCTION

Consumption of electrical energy in the world is constantly growing. Most of the used and produced electrical energy is obtained by the combustion of fossil fuels or by nuclear processes. Thermal power plants and nuclear power plants are natural polluters of the environment. Alternative energy sources that we are surrounded with on the other hand, are pure ecological energy sources. The main alternative energy sources include solar energy, geothermal energy, wind energy, wave energy, bio-energy and hydrogen technologies. One particularly important source of energy is solar energy. Solar energy can play a very important role in providing most of the heating, cooling and electricity needs of the world and also has the potential to solve our environmental problems. The sun is infinite and clean energy source and it sends to earth about 10,000 times as much energy of the world's energy consumption. So, solar energy has attracted a great interest during the last two decades. Converting solar radiation energy into electrical energy and usage of this method of production of the necessary energy becomes an important condition for further development and progress of the planet [1], [2].

Single stage inverters have gained attention, especially in low voltage applications. Different single stage topologies have been proposed, and a comparison of the available interface units is presented [3]. However, the voltage buck properties of the VSI increase the necessity of using a bulky transformer or higher DC voltage. The conventional voltage source inverter is the most commonly used interface units in grid-connected PV system technology due to its simplicity and availability. Several multilevel inverters have been proposed to improve the AC-side waveform quality, reduce the electrical stress on the power switches. The current source inverter has not been extensively investigated for grid-connected renewable energy systems [4], [5].

Grid-connected PV systems using a CSI have been proposed due to DC input current is continuous and system reliability, . The three-phase CSI for PV grid connection proposed in successfully delivered PV power to the grid, without sensing the AC output current, with a total harmonic distortion of 4.5% [6], [7]. However, an AC current loop is essential in the grid-connected application in order to limit the current and quickly recover the grid current variation during varying weather

conditions. A dynamic model and control structure for a single-stage grid connected PV system using a Current source Inverter is proposed. The current injected into the grid has a low THD and unity power factor under various weather conditions. However, the controller consists of only current loops, which affect system reliability.

Dissimilar the three-phase grid-connected CSI, the single-phase system has even harmonics on the DC side, which affect MPPT, reduce the PV lifetime, and are associated with odd order harmonics on the grid side [8]. Therefore, eliminating the even harmonics on the DC side is essential in PV applications [9], [10]. Various techniques have been proposed to reduce the even harmonic effects in CSI PV applications. The conventional solution to the DC current oscillation is to use a large inductor, which is capable of eliminating the even-order harmonics. Practically, the CSI inverter produces high DC current; therefore, an inductor with a large value is usually bulky and large in size [11]. Thus, this technique is practically unacceptable. To eliminate the harmonics without using large inductive, two solutions have been proposed in the literature, namely feedback current control and hardware techniques. Specially designed feedback current controllers intended to eliminate the odd harmonics on the AC side without using large inductance are proposed in the literature. In, the oscillating power effect of the grid is minimized by employing a tuned proportional resonant controller at the third harmonic. The carrier signal is varied with the second-order harmonic component in the DC-link current to eliminate its effect on the current grid. These techniques are not suitable for a single-stage grid connected PV system, because the DC current oscillation is large, which causes high system losses and reduces its lifetime. In the hardware solution proposed in, second order harmonics are eliminated by using an additional parallel resonant circuit on the DC-side inductor. The Arduino controller provides the fast switching operation. LDR sensor is used to track the maximum power in a relatively short time. Even though the hardware solution adds costs, and size, it is considered to be a practical solution for CSI-based PV systems [12], [13].

In this paper, a single-phase grid connected PV system based CSI is proposed. A doubled tuned resonant parallel circuit is also proposed to eliminate the second and fourth order harmonics on the DC side. FLC is used in tracking the MMPT and also manual tracking is achieved with the X axis of the solar panel by Arduino controller.

2 CURRENT SOURCE INVERTER TOPOLOGY

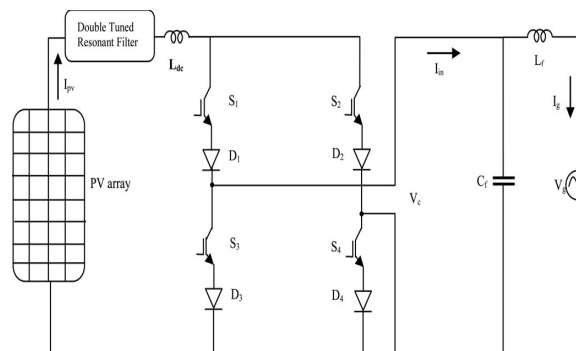


Fig. 1. Single-phase grid connected current source inverter

A single phase transformer less load connected PV system using a CSI is shown in Fig. 1. The inverter has four insulated gate bipolar transistors IGBTs (S1–S4) and four diodes (D1–D4). Each diode is connected in series with an IGBT switch for reverse blocking capability. To eliminate the switching harmonics, a CL filter is connected into the inverter AC side. Two LDR is fixed on the two ends of the solar panel to track the maximum power obtained from the solar cells. In a single phase CSI, the pulsating instantaneous power of twice, the system frequency generates even harmonics in the DC link current [14]. Undesirably, these even harmonics affect MPPT on PV system applications and reduce the PV lifetime. These harmonics reflect onto the AC side as low order odd harmonics in the current and voltage. The filter is capable of smoothing the DC-link current by using relatively small inductances [15]. Even though the impact of the second-order harmonic is significant in the DC-link current, the fourth-order harmonic can also affect the DC-link current, especially when the CSI operates at high modulation indices. To reduce the necessary DC-link inductance, a parallel resonant circuit tuned to the second-order harmonic is employed in series with the DC-link inductor. Therefore, in an attempt to improve the parallel resonant circuit, this paper proposes a double-tuned parallel resonant circuit tuned at the second- and fourth-order harmonics, as shown in Fig. 2.

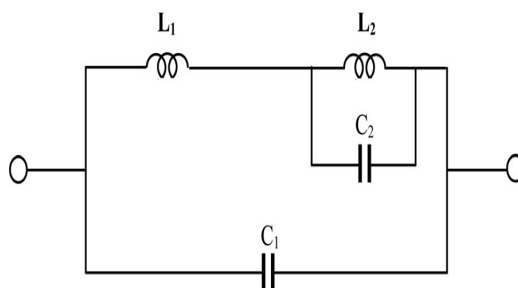


Fig. 2. Double-tuned resonant filter

In order to tune the resonant filter the harmonic frequency, the impedance of C1 and the total impedance of L1, L2, and C2 should have the values of opposite sign. Thus we assume the component resistances are small, and thus can be neglected in the calculating procedure. The capacitances are represented by the following equations:

$$C_1 = \frac{L_2 C_2 - \frac{1}{\omega^2}}{\omega^2 L_1 L_2 C_2 - L_1 - L_2} \tag{1}$$

$$C_2 = \frac{-L_2}{\frac{L_2}{C_1} - \omega^2 L_1 L_2} + \frac{1}{\omega^2 L_2} \tag{2}$$

Where C1 and C2 are the resonant filter capacitances, L1 and L2 are the resonant filter inductances, ZC1 is C1 impedance, Zt is the total impedance of L1, L2, and C2, and ω is the angular frequency. By selecting the inductance values, which are capable of allowing the maximum di/dt at rated current, the angular frequency of the second harmonics and the angular frequency of the fourth harmonic are used. The filter is capable of eliminating both the second- and fourth-order harmonics.

To select the optimum values for the proposed filter components, the effects of varying resonant circuit inductance are analyzed.

3 MODIFIED CARRIER BASED PWM

The Modified carrier-based pulse width is proposed to control the switching pattern of CSI. To provide a continuous path for the DC-side current and one bottom be turned ON during every switching period -circuit current after every active switching action. To understand the switching patterns of the proposed CPWM, is divided into ten regions (t1 – t10), and each region represents one carrier period.

Table 1. Switching combination sequence

Region	Combination Sequence
t ₁	(S ₁ -S ₃) (S ₁ -S ₄) (S ₂ -S ₄) (S ₁ -S ₄)
t ₂	(S ₁ -S ₃) (S ₁ -S ₄) (S ₂ -S ₄) (S ₁ -S ₄)
t ₃	(S ₁ -S ₃) (S ₁ -S ₄) (S ₂ -S ₄) (S ₁ -S ₄)
t ₄	(S ₁ -S ₃) (S ₁ -S ₄) (S ₂ -S ₄) (S ₁ -S ₄)
t ₅	(S ₁ -S ₃) (S ₁ -S ₄) (S ₂ -S ₄)
t ₆	(S ₁ -S ₃) (S ₂ -S ₄) (S ₂ -S ₄) (S ₂ -S ₃)
t ₇	(S ₁ -S ₃) (S ₂ -S ₄) (S ₂ -S ₄) (S ₂ -S ₃)
t ₈	(S ₁ -S ₃) (S ₂ -S ₄) (S ₂ -S ₄) (S ₂ -S ₃)
t ₉	(S ₁ -S ₃) (S ₂ -S ₄) (S ₂ -S ₄) (S ₂ -S ₃)
t ₁₀	(S ₁ -S ₃) (S ₂ -S ₄) (S ₂ -S ₄)

Table 1 shows the switch combination for each of the ten regions. The CSI is operating in an island mode and has the following specification. The DC voltage V_{dc} is 50 V; in the double-tuned resonant filter $L1 = 10$ mH, $L2 = 5$ mH, $C1 = 125$ μ F, and $C2 = 250$ μ F, the capacitor on the AC side is 20 μ F, the inductance is 1 mH, the resistive load is 50 Ω , the output voltage is 110 V, and the switch frequency is 4 kHz.

4 FUZZY LOGIC CONTROL TECHNIQUE

To design a grid connected PV system using a CSI, the relationship between the PV output voltage and the grid voltage by neglecting inverter losses, the PV output power is equation,

$$V_{PV}I_{PV} = \frac{1}{2}I_{g,peak}V_{g,peak} \cos \theta \quad (3)$$

Where θ is the phase angle, V_{PV} and I_{PV} are the PV output voltage and current, respectively, while $V_{g,peak}$ and $I_{g,peak}$ are the grid peak voltage and current, respectively. The current is equal to the Photovoltaic output current multiplied by the inverted index M

$$I_{g,peak} = MI_{PV} \quad (4)$$

These equations describing the relationship between the solar output voltage and the grid voltage are, therefore, in order to interface the PV system to the grid using a CSI, the PV voltage should not exceed half the grid peak voltage [16]. The CSI is utilized to track the PV MPP and to interface the PV system to the grid. In order to achieve these requirements, three control loops are employed, namely MPPT, an AC current loop, and a voltage loop. To operate the PV at the MPP, MPPT is used to identify the optimum grid current peak value. Any conventional MPPT technique can be used [17], [18]. However, to prevent significant losses in power, the tracking technique should be fast enough to handle any variation in load or weather conditions. Therefore, a fuzzy logic controller (FLC) is used to quickly locate the MPP [19].

The inputs of the FLC are

$$\Delta P = P(K) - P(K-1) \quad (5)$$

$$\Delta IPV = IP(K)V - IP(K-1)V \quad (6)$$

The output Equation is

$$\Delta I_{g,ref} = I_{g,ref}(k) - I_{g,ref}(K-1) \quad (7)$$

Where ΔP and ΔIPV are the PV array output power and current change, As mentioned before, all machines can process crisp or classical data, such as either '0' or '1'. In order to enable machines to handle vague language input such as 'Somehow Satisfied', the crisp input and output must be converted to linguistic variables with fuzzy components [20]. $\Delta I_{g,ref}$ is the grid current amplitude change reference, $I_{g,ref}$ is the grid current reference, and k is the sample instant. The variable inputs and output are divided into four fuzzy subsets: PB (Positive Big), NB (Negative Big), PS (Positive Small) and NS (Negative Small). To operate the fuzzy combination, a Mamdani's method is used. The behavior found on the controller input and the output, the shapes and fuzzy subset partitions of the membership function of both input and output are shown in Fig. 3.

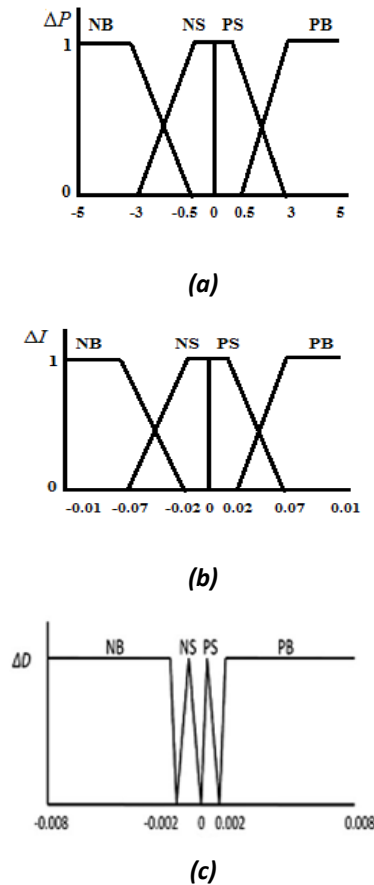


Fig. 3. Membership function: (a) input ΔP , (b) input ΔI , and (c) output ΔD

To ensure synchronization between the grid current and voltage, a sinusoidal signal generated by a phase-locked-loop (PLL) is multiplied by the MPPT output. The Fuzzy Logic Controller provides the constant high power by comparing it with the value taken before 5 seconds. Thus, every five seconds the controller checks it for the deviation of the change in power to maintain the maximum power from the panel for precise control of the single-phase inverter, proportional Arduino controller is employed in the voltage and current loop controllers. The block diagram of the FLC based MPPT is shown in Fig. 4.

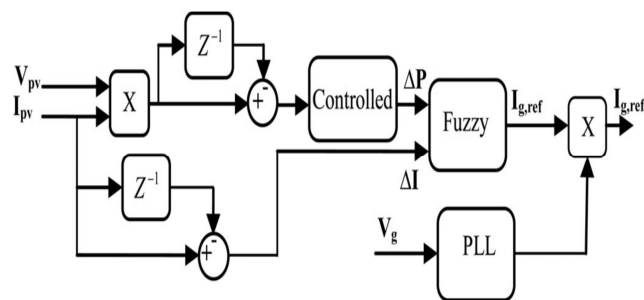


Fig. 4. Block diagram of the FLC-based MPPT

The fuzzy subset duty cycle changes in real numbers

$$\Delta I_{g,ref} = \frac{\sum_i^n \mu(I_{g,ref,i}) I_{g,ref,i}}{\sum_i^n \mu(I_{g,ref,i})} \quad (8)$$

Where $\Delta I_{g,ref}$ is the fuzzy controller output and $\Delta I_{g,ref}$ is the center of composition at the output membership function. To ensure synchronization between the grid current and voltage, a sine signal generated by a phase-locked-loop (PLL) is multiplied by MPPT output.

5 ARDUINO CONTROLLER

The Arduino is a microcontroller board based on the ATMEGA328. It has 14 digital input/output pins (of which 6 can be used as PWM outputs), 6 analog inputs, a 16 MHz ceramic resonator, a USB connection, a power jack, an ICSP header, and a reset button. It contains everything needed to support the microcontroller; simply connect it to a computer with a USB cable or power it with AC-to-DC adapter or battery to get started. The Uno differs from all preceding boards in that it does not use the FTDI USB-to-serial driver chip. Instead, it features the Atmega16U2 (Atmega8U2 up to version R2) programmed as a USB-to-serial converter.

6 SIMULATION ANGLE

In this PV module with a total rated power of 500W are tested in the proposed system. The AC-side filter capacitor is selected to attenuate high frequency harmonics that are associated with switching frequencies and their side bands, taking into account the rated AC and DC currents. So that rated power, the converter is able to supply the AC side active and reactive power demands, and compensate for filter capacitor and inductor reactive power, without sliding into over modulation. The results of the proposed system under normal weather conditions are shown in Fig. 5.

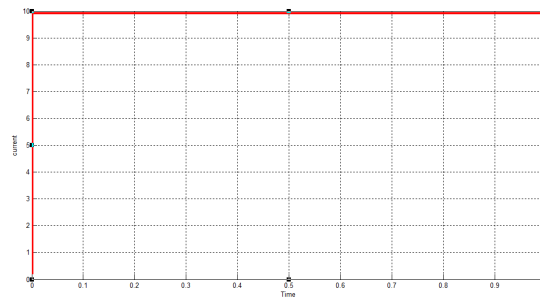


Fig. 5. PV Current

The point at which the maximum voltage and maximum current is reached is the maximum power point. The maximum power is maintained at 24 watts. Due to the variation in intensity of the light the maximum power is also varied, but the tracking system maintains the PV maximum power extracted in a relatively short time with small oscillation in steady state, as shown in Fig.6.

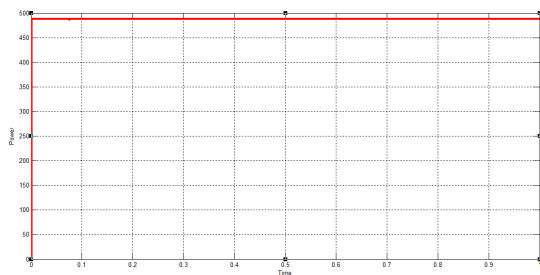


Fig. 6. PV Power

Fig.7 shows that the CSI output current is not violated, by allowing switching of one current level at the same time. In the CSI-based PV system, the controller's task is to control the DC-side current. It is observed that the range of variation in the DC-side current of CSI during fault is tightly limited due to the regulatory role of the DC-side current controller.

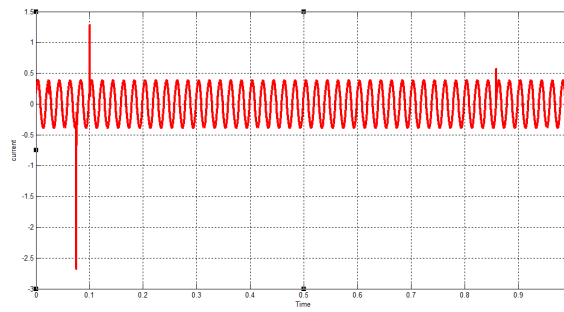


Fig. 7. CSI output current

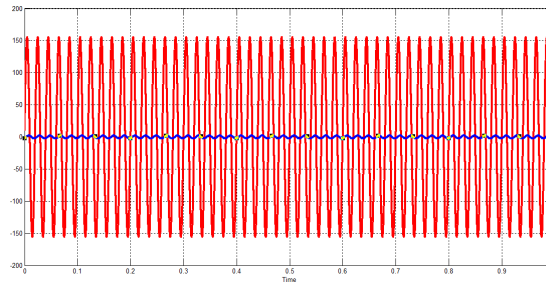


Fig. 8. Grid Voltage and Current waveform

The grid voltage and current are shown in Fig. 8 where both are synchronized and the THD of the grid current is only 1.5%. In addition, the grid active power and reactive power are shown in Fig. 9. The total system efficiency is 95%, and the power factor is almost unity.

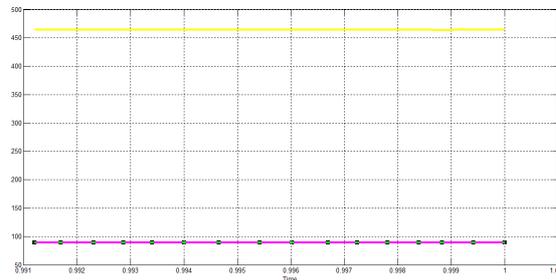


Fig. 9. Real and Reactive Power waveform

The current flowing into the grid was filtered to resemble a pure sine wave in phase with the grid voltage. As I_{grid} is almost a pure sine wave at unity power factor, the total harmonic distortion (THD) can be reduced compared with the THD. Where both are synchronized and the THD of the grid current is only 1.5%. The Fig. 10 shows the efficiency level of the system. The Fuzzy Logic Controller increases the Efficiency of the system to 72.5%. Stepper motor used for the direction control gives a precise position control and MPP is tracked efficiently throughout the day with the change in sun position.

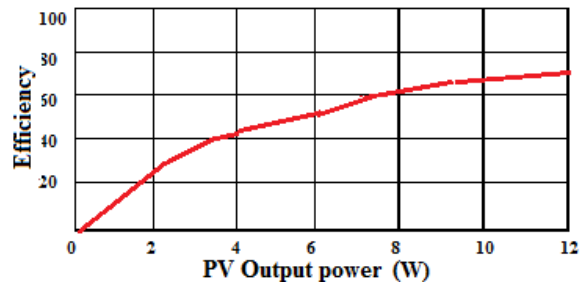


Fig. 10. Efficiency with PV output power

The Fig.10 shows the efficiency level of the system. The Fuzzy Logic Controller increases the Efficiency of the system to 72.5%. Stepper motor used for the directional control gives a precise position control and MPP is tracked efficiently throughout the day with the change in sun position. The design specifications and circuit parameters and parameters of the DC-side tuned filter is given in Table 2.

Table 2. Specifications and Parameters

S. No.	Description	Value
1	PV open circuit voltage, Voc(V)	80
2	PV Short circuit current, I _{sc} (A)	15
3	PV array rated power, P _R (W)	500
4	Resonant filter inductor, L ₁ (mH)	10
5	Resonant filter inductor L ₂ (mH)	5
6	Resonant filter capacitor C ₁ (μF)	125
7	Resonant filter capacitor C ₂ (μF)	250
8	DC link inductor, L _{dc} (mH)	5
9	Switching frequency, F _s (KHz)	4
10	AC line inductor, L(mH)	1
11	AC line capacitor, C(μF)	20

7 EXPERIMENTAL RESULTS

The performance of the proposed Fuzzy logic based Current Source Inverter with experimental models of the solar cell movement systems with a mechanical assemble to move the panel from 180° East to West is verified experimentally is shown in Fig 11. The experimental setup consists of a solar array panel to emulate PV system operational track the maximum power point, and interface the PV system to the Load. An Arduino Microcontroller is used to generate the PWM signals and realize the proposed feedback loop controllers. The solar tracking parameters are shown in Table.3.

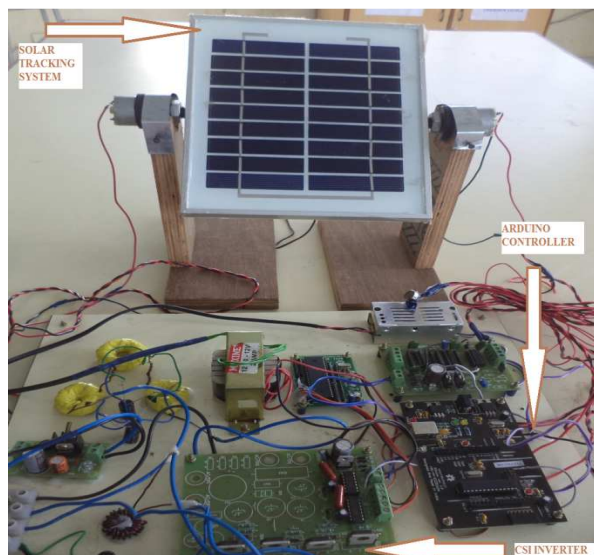


Fig. 11. Experimental setup for solar tracking

7.1 SOLAR PANEL OUTPUT VOLTAGE

The rating of the Solar panel is 10 Volts. The Maximum voltage obtained from the solar Panel is 8.7 volts. Based on dividing the voltage into four values of fuzzy the output voltage will be decided to one crisp value. The Maximum power point is identified with rules framed in fuzzy. The open circuit voltage and short circuit current is 11.2V and 0.37A respectively. The MPPT successfully locks the DC Voltage to the optimum value.

7.2 CURRENT SOURCE INVERTER OUTPUT VOLTAGE

The output voltage of the inverter is about 8 volts. The optimum PV voltage is attained in a relatively short time. Also the CSI successfully injects the PV current into the load with low total harmonic distortion. The output of an inverter voltage is a pure sine wave when increase the input voltage can achieve the same. For the experimental setup of the mechanical system, the panel rating is kept at 12 volts. Due to the Transformer less inverter circuit topology the output voltage is not a boost voltage. When the similar solar arrays are connected in series to produce the desired voltage rating

7.3 AUTOMATIC SINGLE AXIS TRACKING

The solar panel rotates based on the light incident on the LDR sensor. In order to track the sun trajectory, a horizontal axis tracker with a 12V PV panel was shown in Fig.11. The panel is tilted around the horizontal axis using DC motor connected to the panel through a gear with a 10 revolution per minute. The tracker is controlled using a two LDR sensor. The sensors are configured in a way that LDR1 and LDR2 are used to track the sun horizontally. When one receives more light than the other, the panel is not aligned properly and an error voltage results. The error voltage is used as a command to an amplifier circuit to drive the motor and align the Panel to be perpendicular to the light source beam.

Table 3. Solar Tracking Parameters

S. No.	Description	Value
1	PV open circuit voltage, V_{oc}	11.2 V
2	PV Short circuit current, I_{sc}	0.37A
3	PV Rating of the panel	12V
4	Maximum voltage obtained	8.7V
5	Inverter output voltage	8V

8 CONCLUSION

A single phase grid connected PV system using a CSI has been implemented that could meet the load requirements without using a high DC voltage or a bulky transformer. Since the system consists of a single-stage, the PV power is delivered to the load with high efficiency, low cost, and small footprint. Moreover, the THD of the grid injected current was 0.04% in the simulation results. The controller has been combined with the solar tracking system and the control was realized with the fuzzy logic controller. Fuzzy logic demonstrates efficient control, faster response and better conversion of human/ operator knowledge. The result also shown a better output over the conventional methods, Arduino UNO turned out to be an easy platform implement the control strategy. LDR resistors are used to determine the solar light intensity. Sun tracking, the generating power system is designed and implemented in real time. The sun tracking controller and the controller for grid-connected photovoltaic system are tested using MATLAB/Simulink environment. The proposed FLC shows excellent result and the solar tracking power generation with fuzzy controller is able to track the sunlight automatically. It is an efficient system for solar energy collection.

REFERENCES

- [1] J. S. Choi, D. Y. Kim, K. T. Park, C. H. Choi and D. H. Chung, "Design of Fuzzy Controller Based on PC for Solar Tracking System", International Conference on Smart Manufacturing Application, pp.9-11, April 2008.
- [2] A. Mehrizi-Sani and R. Iravani, "Potential-function based control of a microgrid in islanded and grid-connected modes," IEEE Trans. Power Syst., Vol. 25, No. 4, pp. 1883–1891, Nov. 2010.
- [3] W. Fei, J. L. Duarte, and M. A. M. Hendrix, "Grid-interfacing converter systems with enhanced voltage quality for microgrid application-concept and implementation," IEEE Trans. Power Electron., Vol. 26, No. 12, pp. 3501–3513, Dec. 2011.
- [4] S. Dasgupta, S. K. Sahoo, S. K. Panda, and G. A. J. Amaratunga, "Single- phase inverter-control techniques for interfacing renewable energy sources with microgrid—Part II: Series-connected inverter topology to mitigate voltage-related problems along with active power flow control," IEEE Trans. Power Electron., Vol. 26, No. 3, pp. 732–746, Mar. 2011.
- [5] A. Louchene, A. Benmakhlouf and A. Chaghi, "Solar Tracking System with Fuzzy Reasoning Applied to Crisp Sets", Revue des Energies Renouvelables, Vol. 10, No.2, pp. 231 – 240, 2007.
- [6] W. Tsai-Fu, C. Chih-Hao, L. Li-Chiun, and K. Chia-Ling, "Power loss comparison of single- and two-stage grid-connected photovoltaic systems," IEEE Trans. Energy Convers., Vol. 26, No. 2, pp. 707–715, Jun.2011.
- [7] S. B. Kjaer, J. K. Pedersen, and F. Blaabjerg, "A review of single-phase grid-connected inverters for photovoltaic modules," IEEE Trans. Ind. Appl., Vol. 41, No. 5, pp. 1292–1306, Sep.–Oct. 2005.
- [8] N. Barsoum, "Implementation of a prototype for a traditional solar tracking system", Third UKSim European Symposium on Computer Modeling and Simulation, 2009.
- [9] B. Sahan, S. V. Araujo, C. No`ding, and P. Zacharias, "Comparative evaluation of three-phase current source inverters for grid interfacing of distributed and renewable energy systems," IEEE Trans. Power Electron., Vol. 26, No. 8, pp. 2304–2318, Aug. 2011.
- [10] B. Sahan, A. N. Vergara, N. Henze, A. Engler, and P. Zacharias, "A single-stage PV module integrated converter based on a low-power current-source inverter," IEEE Trans. Ind. Electron., Vol. 55, No. 7, pp. 2602–2609, Jul, 2008.
- [11] S. Busquets-Monge, J. Rocabert, P. Rodriguez, S. Alepuz, and J. Bordonau, "Multilevel diode-clamped converter for photovoltaic generators with independent voltage control of each solar array" IEEE Trans. Ind. Electron., Vol. 55, No. 7, pp. 2713–2723, Jul. 2008.
- [12] R. T. H. Li, H. S. -H. Chung, and T. K. M. Chan, "An active modulation technique for single-phase grid-connected CSI" IEEE Trans. Power Electronics., Vol. 22, No. 4, pp. 1373–1382, Jul. 2007
- [13] S. Nonaka, "A suitable single-phase PWM current source inverter for utility connected residential PV system" Sol. Energy Mater. Sol. Cells, Vol. 35, pp. 437–444, Sep. 1994.
- [14] W. Tsai-Fu, C. Chih-Hao, L. Li-Chiun, and K. Chia-Ling, "Power loss comparison of single- and two-stage grid-connected photovoltaic systems" IEEE Trans. Energy Convers., Vol. 26, No. 2, pp. 707–715, Jun. 2011.
- [15] Guo, Y.Z., Cha, J.Z., Liu, W. and Tian, Y.B. A System Modeling Method for Optimization of a Single Axis Solar Tracker. ICCASM 2010.
- [16] Y. Chen and K. Ma-Smedley, "A cost-effective single-stage inverter with maximum power point tracking," IEEE Trans. Power Electron., Vol. 19, No. 5, pp. 1289–1294, Sep. 2004.
- [17] T. J. Liang, Y. C. Kuo, and J. F. Chen, "Single-stage photovoltaic energy conversion system," Proc. Inst. Elect. Eng., Vol. 148, No. 4, pp.339–344, 2001.

- [18] B. M. T. Ho and H. S.-H. Chung, "An integrated inverter with maximum power tracking for grid-connected power systems" IEEE Trans. Power Electron., Vol. 20, No. 4, pp. 953–962, Jul. 2005.
- [19] B. K. Bose, P. M. Szezesny, and R. L. Steigerwald, "Microcontroller control of residential photovoltaic power conditioning system" IEEE Trans. Ind. Appl., Vol. 21, No. 5, pp. 1182–1191, Sep./Oct. 1985.
- [20] I. Anton, F. Perez, I. Luque, and G. Sala, "Interaction between Sun tracking deviations and inverter MPP strategy in concentrators connected to grid" in Proc. IEEE Photovolt. Spec. Conf., pp. 1592–1595, 2002.